REGULAR PAPER

Large critical field of Li-doped NiO investigated by p^+-NiO/n^+-Ga_2O_3 heterojunction diodes

To cite this article: Katsunori Danno *et al* 2023 *Jpn. J. Appl. Phys.* **62** SF1007

Japanese Journal of Applied Physics **62**, SF1007 (2023) **REGULAR PAPER**
https://doi.org/10.35848/1347-4065/acb2d7

Large critical field of Li-doped NiO investigated by p^+-NiO/n^+-Ga_2O_3 heterojunction diodes

Katsunori Danno*, Motohisa Kado, Toshimasa Hara, Tatsuki Takasugi, Hayate Yamano, Yusuke Umetani, and Tetsuya Shoji

Toyota Motor Corporation, Higashifuji Technical Center, 1200, Mishuku, Susono, Shizuoka, 410-1193, Japan

*E-mail: katsunori_danno@mail.toyota.co.jp

Received November 29, 2022; revised January 9, 2023; accepted January 13, 2023; published online February 14, 2023

Critical electric fields (E_C) of lithium-doped p^+-nickel oxide (NiO) were investigated by the capacitance (C)–voltage (V) and current (I)–V measurements using p^+-NiO/n^+-gallium oxide (Ga_2O_3) heterojunction diodes. The E_C was estimated by device simulations using the net acceptor concentrations (N_A) obtained from C–V measurements and breakdown voltages obtained from reverse I–V characteristics. The E_C of NiO depended on the N_A of the NiO and ranged from 5.4 to 10.1 MV cm^{-1}. Large E_C was obtained for high N_A. NiO was confirmed to be one of the promising p-type oxides to realize high-power p-n heterojunction devices with Ga_2O_3 due to the high E_C.

1. Introduction

Gallium oxide (Ga_2O_3) is an attractive semiconductor material for developing high-power devices, owing to its superior properties such as wide bandgap of 4.6–4.9 eV, high breakdown field of 8 MV cm^{-1}, and relatively high electron mobility of 300 cm^2 $V^{-1}s^{-1}$.[1–5] Particularly, its monoclinic beta-phase Ga_2O_3 (β-Ga_2O_3) has been regarded as the most promising polymorphs for vertical type high-power devices, due to its thermal stability and availability on large diameter substrates.[3]

To realize high-performance and reliable power devices, in general, both n- and p-type semiconducting materials are required. Although n-type conductivity of Ga_2O_3 has been realized over many orders of magnitude by doping with shallow donors such as tin (Sn) and silicon (Si),[6,7] a p-type conductivity has remained not been fully developed due to the absence of shallow acceptors[8] and lack of natural formation of self-trapped holes in Ga_2O_3.[9,10]

Thus, the use of p-type oxides is a potential alternative strategy to form a p-n heterojunction with Ga_2O_3. Nickel oxide (NiO) is one of the promising p-type oxides to realize high-power p-n heterojunction devices with Ga_2O_3 due to the relatively large bandgap of 3.4–3.7 eV[11] and availability of epitaxial NiO layers on Ga_2O_3 substrates.[12]

Though the bandgap of NiO is larger than other p-type oxides, the reported values are smaller than that of Ga_2O_3. Consequently, the critical electric field (E_C) of NiO is expected to be smaller than that of Ga_2O_3, limiting the electrical performances such as breakdown voltage (V_B) of NiO/Ga_2O_3 heterojunction devices. Moreover, the E_C of moderately doped NiO is expected to be lower than 4 MV estimated from other p-type semiconductors with similar bandgaps such as SiC (3.3 eV) and GaN (3.4 eV). On the other hand, experimentally V_B of more than 1 kV could be obtained for NiO/Ga_2O_3 heterojunction diodes.[13–18] Recently, a large V_B of 8.32 kV[18] was also reported for a NiO/Ga_2O_3 heterojunction diode. The electric field at the V_B (breakdown field; E_B) was calculated to be 4.9 MV cm^{-1} at the NiO/Ga_2O_3 heterojunction, which is higher than E_C estimated from the bandgap on NiO mentioned above. Consequently, if a highly doped NiO was employed for the heterojunction diodes, E_C might be increased as in the case of Si and SiC.[19] As a result, very high E_B at the p-n junction might be obtained. Thus, estimation of E_C of NiO, especially for highly doped NiO, is required for the design of high-voltage NiO/Ga_2O_3 heterojunction devices. However, doping concentration dependence of E_C of NiO has not been established yet as far as the authors know.

In this work, we investigated the E_C of highly doped NiO by varying the doping concentration from 3.8×10^{18} to 4.8×10^{19} cm^{-3}, by using p^+–NiO/n^+-Ga_2O_3 diodes.

2. Experimental methods

To investigate the E_C, p^+-NiO/n^+-Ga_2O_3 diodes were fabricated as shown in Fig. 1. The advantages of using n^+-Ga_2O_3 substrates for the diodes are as follows: first, the net acceptor concentration (N_A) of p^+–NiO layers can be estimated by the capacitance (C)—voltage (V) measurements. In the case of p^+–NiO/n^-–Ga_2O_3 diodes, C is mainly determined by the net donor concentration (N_D) of n^--Ga_2O_3, which is much smaller than N_A. It is difficult, therefore, to estimate the N_A of the p^+-NiO layer precisely. On the other hand, N_A can be estimated by C–V measurements using p^+–NiO/n^+-Ga_2O_3 diodes. The details will be discussed in Sect. 3.1. Second, is related to the estimation of V_B. In the case of p^+-NiO/n^+–Ga_2O_3 diodes, breakdown occurs at a much lower voltage than that in p^+-NiO/n^--Ga_2O_3 diodes. Moreover, the depletion layer width at the V_B can be kept small due to highly doped NiO and Ga_2O_3. By employing mesa structure diodes with a mesa height to be large enough compared to the depletion layer width, one-dimensional electric field distribution in an abrupt junction can be obtained without electric field crowding at the mesa corner. Thus, E_B of the p^+-NiO/n^+-Ga_2O_3 junction, which relates to E_C on NiO, can be obtained by simple mesa structure diodes.

Sn-doped n^+- Ga_2O_3 (001) substrates used in the diode were fabricated by edge-defined film-fed growth method.[3] The N_D of the substrates was 9.1×10^{18} cm^{-3}. At first, backside ohmic contact of titanium (Ti)/aluminum (Al) (50/100 nm) was formed by sputtering followed by rapid thermal annealing (RTA) at 500 °C under nitrogen (N_2) ambient for 5 min.

Then, p^+-NiO layer with a thickness of 100–140 nm was deposited by sputtering on the n^+- Ga_2O_3 (001) substrates. NiO was doped with lithium (Li), which acts as a shallow acceptor in NiO.[20,21] Sputtering of Li-doped NiO was

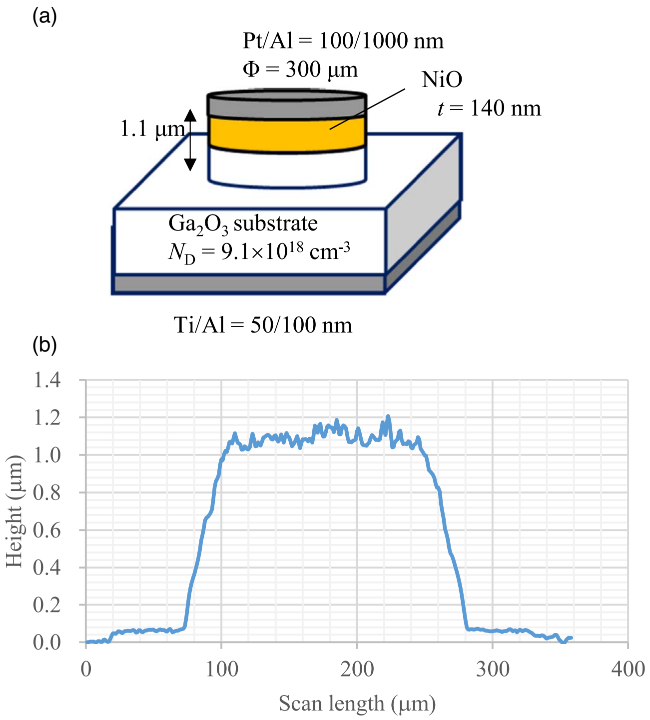

Fig. 1. (Color online) (a) Schematic structure of NiO/Ga_2O_3 diode used for characterization of N_A and E_B of NiO. (b) Height profile of the mesa structure diode with a diameter of 200 μm obtained with profilometer.

performed by using 0–10 atomic percent (at%) Li-doped NiO targets without intentional heating at a pressure of 0.2 Pa. Oxygen (O_2)/argon (Ar) mixture gas was used for the sputtering where typical O_2 partial pressure was 60%.

Prior to mesa formation, ohmic contact for NiO was formed by sputtering of platinum (Pt)/Al (100/1000 nm) through a metal mask. The typical diameter of the contacts used for the characterization of electronic properties was 300 μm. The contacts were also utilized as metal masks for reactive ion etching (RIE) performed for the formation of mesa structures.

RIE was performed with radio frequency plasma (600 W) under SF_6 (15 sccm) and Ar (5 sccm) flow at 1.5 Pa for 20 min. No special treatment such as surface passivation was not applied to the structure. A mesa structure with a height of 1.0–1.2 μm was formed by RIE. Figure 1(b) shows the height profile of a mesa structure diode with a diameter of 200 μm obtained by a profilometer. Mesa height including Pt contact (thickness: 100 nm, Al contact was removed) was approximately 1.1 μm. In order to suppress the electric field crowding of fabricated diodes, the mesa height of Ga_2O_3 was designed to be larger than the depletion layer width when the V_B was applied to the diodes.

The crystallinity of a NiO layer was investigated by scanning transmission electron microscopy (STEM). We performed C–V measurements of the diodes for the estimation of N_A of NiO and current (I)–V measurements for V_B. By using the results obtained above, the E_B of p^+-NiO/n^+-Ga_2O_3 diodes was calculated with a device simulation (TCAD Sentaurus Device).

3. Results and discussion

3.1. Results

At first, the crystal structure of a NiO layer was investigated by bright field STEM. The NiO layer observed here was formed by sputtering with a 10at%Li-doped NiO target. The specimen for STEM observation of the (100) cross section was prepared by a focus ion beam. Figure 2 shows a cross-sectional STEM image near the interface between p^+-NiO and n^+-Ga_2O_3. As shown in Fig. 2, crystalline arrays were observed in the NiO layer near the interface. At the early stage of the sputtering, therefore, NiO epitaxial layer might have grown. Generally, the crystallinity of NiO around the interface is important for reverse characteristics of p^+-NiO/n^+-Ga_2O_3 diodes such as V_B and leakage current because the electric field becomes maximum at the interface.

The N_A of NiO layers was investigated by C–V measurement of p^+-NiO/n^+-Ga_2O_3 diodes under 1 MHz. Figure 3 shows C–V characteristics of a p^+–NiO/n^+–Ga_2O_3 diode, the NiO layer of which was prepared by sputtering using a 1at%Li-doped NiO target. The C of the p-n heterojunction diode is given by

$$C = \left[\frac{e\varepsilon_0\varepsilon_n\varepsilon_p N_D N_A}{2(\varepsilon_n N_D + \varepsilon_p N_A)}\right]^{1/2}(V_{bi} - V)^{1/2}, \quad (1)$$

where e is the elementary charge, ε_0, ε_n and ε_p the permittivity of vacuum, Ga_2O_3(10.0)[22] and NiO(11.9),[23] respectively. The V_{bi} is the built-in potential, which is experimentally obtained from the extrapolation to $1/C^2 = 0$. The value of the diode was 2.4 V. We used N_A as the fitting parameter. The fit of Eq. (1) to experimental $1/C^2$–V plots is presented as the solid line in Fig. 3 while experimental data are plotted by open circles. From the fit, the N_A of the present NiO layer used for the diode was estimated to be 1.9×10^{19} cm^{-3}.

To control the N_A of NiO layers, NiO targets with a various Li concentrations of 0.0 (undoped), 0.1, 1.0, and 10.0at% were used for sputtering. At first, the Li concentration of NiO layers was investigated by secondary ion mass spectrometry (SIMS). Figure 4(a) represents the relation between the Li concentration of the NiO layers and that of the NiO targets. As shown in the figure, the Li concentration of the NiO layers was linearly increased by increasing that of the NiO targets. As shown in Fig. 4(b), the N_A estimated from C–V measurements could be also controlled in the range from 1.1×10^{18} cm^{-3} to 4.8×10^{19} cm^{-3} by changing the Li concentration of the NiO target. Relatively high Li-doping was realized compared to the previous work.[12] Comparing Figs. 4(a) and 4(b), however, the N_A was two orders of magnitude lower than Li concentration for the NiO layers formed with highly Li-doped NiO targets. This implies that

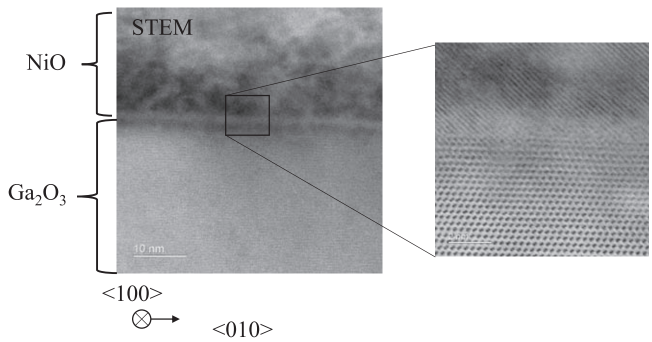

Fig. 2. Cross-sectional STEM image near the interface between p^+-NiO and n^+-Ga_2O_3. 10at%Li-doped NiO target is used for the sputtering of the NiO layer.

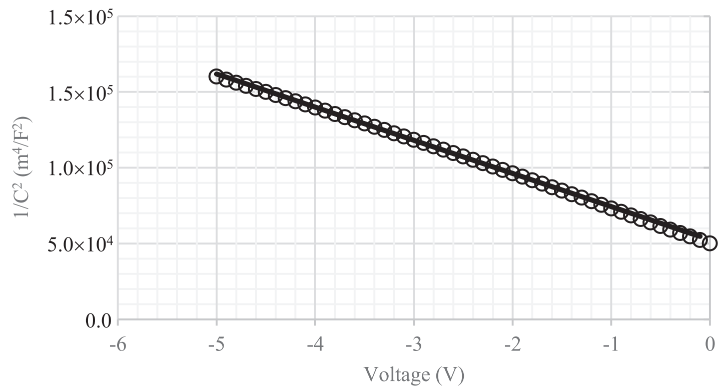

Fig. 3. *C–V* characteristics of the p^+-NiO/n^+-Ga_2O_3 diode, NiO layer of which was prepared by sputtering using 1at%Li-doped NiO target (open circles). Fit for the characteristics is also shown as a solid line.

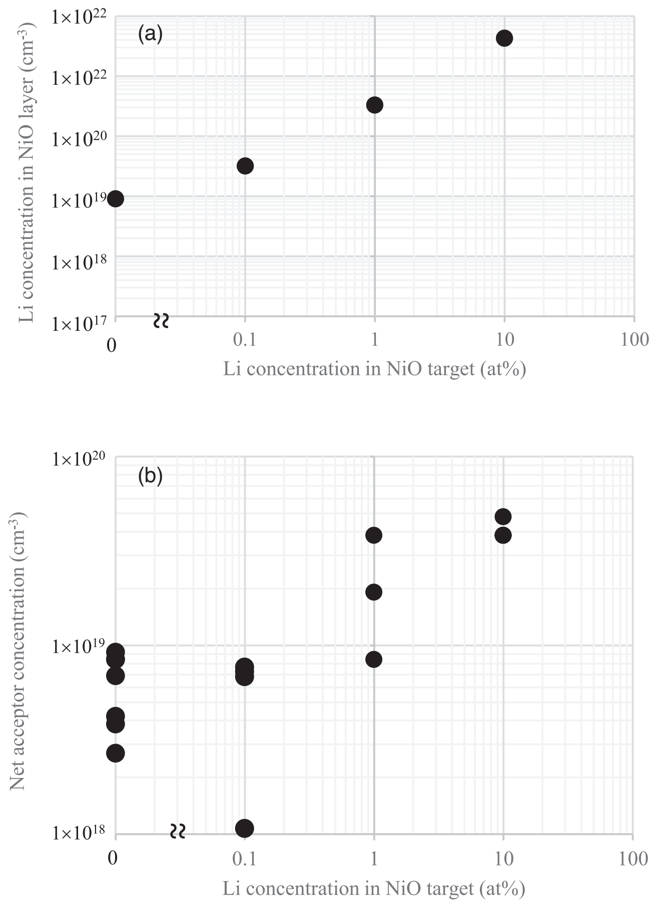

Fig. 4. Dependence of (a) Li concentration and (b) N_A of NiO layers on Li concentration in NiO sputtering target.

only a small number of Li atoms is activated by substituting Ni sites and/or that acceptor is compensated by deep levels. When the Li concentration of the NiO targets was lower than 0.1 at%, on the other hand, the N_A of the NiO layer did not depend on the Li concentration of NiO targets. In the region, the N_A might be determined by residual Li concentration and/or nickel vacancy (V_{Ni}), which act as an acceptor.[21,24,25] Li atoms might be contaminated from a chamber during the sputtering process. Run-to-run and/or in-plan variability in residual Li concentration and/or V_{Ni} concentration may cause scattering of N_A in Fig. 4(b). Reduction of background doping is essential to control doping concentration precisely. Further understanding of the doping mechanism is, therefore, required for the purpose.

To estimate E_B, V_B of p^+-NiO/n^+-Ga_2O_3 diodes shown in Fig. 1 was characterized by *I–V* measurements. Figure 5 shows reverse *I–V* characteristics of a p^+-NiO/n^+-Ga_2O_3 diode obtained at room temperature (RT), 75 °C, and 150 °C. The p^+–NiO layer was formed by sputtering with the 1.0at% Li-doped NiO target, and the N_A of the layer was 1.9×10^{19} cm^{-3} (the same diode with that used for Fig. 3). As shown in Fig. 5, the diode successfully showed a low V_B of 23.1 V at RT. The diode showed higher V_B at the higher temperature (27.8 V for 75 °C and 28.6 V for 150 °C). Thus, increasing of the V_B by increasing the temperature, implies the avalanche breakdown has occurred. Assuming an abrupt junction, the depletion layer width was calculated as approximately 20 nm in the NiO layer and 76 nm in Ga_2O_3 at the breakdown voltage at RT which were smaller than the thickness of the NiO layer (100–140 nm) and mesa height, respectively. It suggests that electric field crowding can be avoided at the mesa corner and that the electric field becomes maximum at the p-n junction. Moreover, the electric-field distribution of the non-punch-through structure was realized since the depletion layer width was much smaller than the thickness of the NiO layer and Ga_2O_3.

To confirm the electric field distribution of the diode mentioned above, the device simulation was conducted by Sentaurus Device [Fig. 6(a)]. A mesa structure diode with a

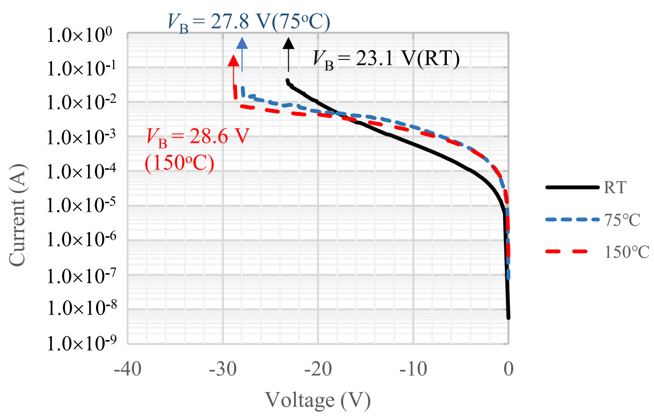

Fig. 5. (Color online) Reverse *I–V* characteristics of p^+-NiO/n^+-Ga_2O_3 diode obtained at RT, 75 °C, and 150 °C. The NiO layer with a N_A of NiO 2.5×10^{19} cm^{-3} was formed with sputtering using 1at%Li-doped NiO target.

small mesa diameter of 2.1 μm was employed for the simulation for convenience although the thickness of NiO and mesa height were almost the same as the fabricated diodes. The electron affinities of 1.8 eV for NiO[26] and 4.0 eV for Ga_2O_3[27] were used for the simulation. By considering the bandgaps of NiO and Ga_2O_3, the conduction band and valence band offsets of the diodes were determined to be 2.2 eV and 3.1 eV, respectively. Interface states at the NiO and Ga_2O_3 interface were not considered. Figure 6(a) shows the electric field distribution of the diode [same as that used in Fig. 5 ($N_A = 1.9 \times 10^{19}$ cm^{-3}, $N_D = 9.1 \times 10^{18}$ cm^{-3})]. For the thickness of the NiO layer, a designed value (100 nm) was used. As shown in Fig. 6(a), the largest electric field was obtained at the p$^+$-NiO/n$^+$-Ga_2O_3 interface. The electric field at the interface was uniform regardless of the position. The depth profile of the electric field of the diode was shown in Fig. 6(b). From Fig. 6(b), the maximum breakdown electric field at V_B (E_B) was confirmed to be 7.7 MV cm^{-1} for the situation.

The N_A dependence of E_B was investigated by reverse *I–V* characteristics of various p$^+$-NiO/n$^+$-Ga_2O_3 diodes. The N_A of p$^+$-NiO layers used for the diodes was changed from 3.8×10^{18} cm^{-3} to 4.8×10^{19} cm^{-3} as shown in Fig. 4(b), while the N_D of Ga_2O_3 was kept constant at 9.1×10^{18} cm^{-3} for all diodes investigated in this report. For the diodes used here, V_B was in the range between 23.1 to 34.7 V. The depletion layer widths of the NiO layer and Ga_2O_3 were smaller than the NiO layer width and mesa height for the diodes under the reverse bias conditions. From the V_B obtained by *I–V* measurements, N_A of the NiO layers, and N_D of the Ga_2O_3 substrates, E_B of the diodes was estimated by the device simulations as mentioned above. Figure 7 shows the relation between E_B and N_A of the NiO layers. The E_B was increased by increasing N_A, and reached 10.1 MV cm^{-1}. The increase of E_B is probably brought from the increase of E_C of NiO, resulting from the increase of N_A of the NiO layer. Since the N_D of Ga_2O_3 was almost constant for all diodes used here, Ga_2O_3 was most likely not responsible for the change of E_B. Therefore, we believe that E_B corresponds to the E_C of NiO layers. It also implies that avalanche breakdown occurred not in n$^+$-Ga_2O_3, but in p$^+$-NiO layers at the p-n interface. The E_B at the interface was higher than 8 MV cm^{-1}, which was higher than the reported E_C value for Ga_2O_3.[2] Because the N_D of the Ga_2O_3 used here was as high as 9.1×10^{18} cm^{-3}, the E_C of Ga_2O_3 might have also been increased.

This dependency of E_C on doping concentration was also observed in the past for Si and SiC.[19] It is reported that the width of the space charge region decreases for the highly doped layer. It is worth noting that in this study N_A is high in the NiO layer. As a result, carriers in the NiO layer are less accelerated by the applied electric field compared with low N_A. In other words, mobility might be reduced for highly doped NiO due to impurity scattering. This is a reason why a large E_C can be obtained for the highly doped NiO layers.

3.2. Discussion

From Fig. 7, the E_C of NiO can be experimentally approximated by the relationship,

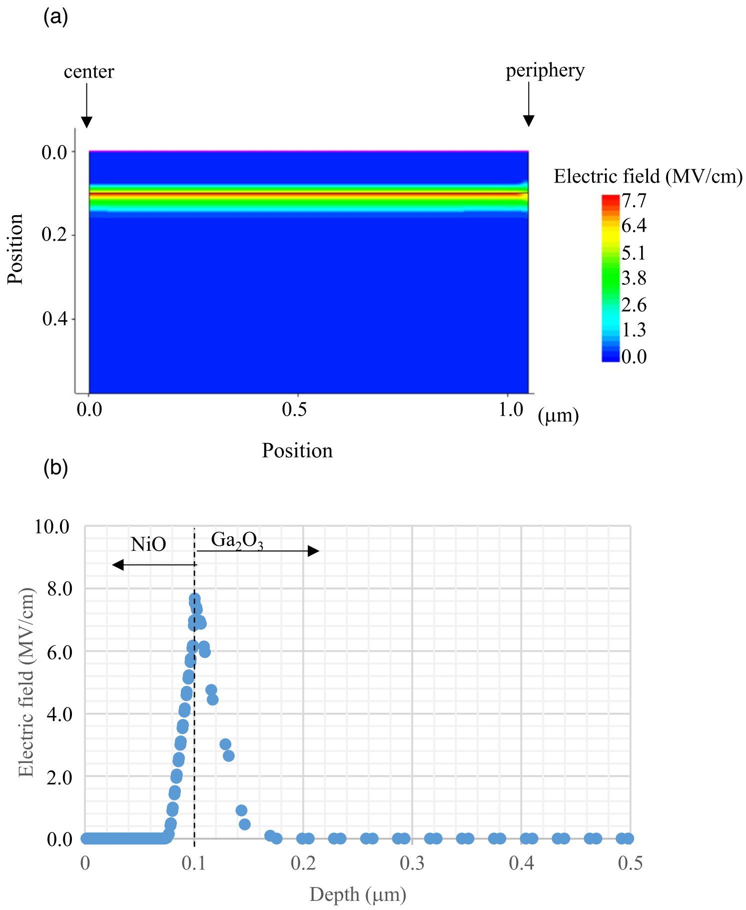

Fig. 6. (Color online) (a) Electric field distribution of NiO/Ga_2O_3 diode at breakdown voltage. The diode with a small mesa diameter of 2.1 μm was used for the calculation for convenience. (b) Relation between electric field and depth from the diode surface.

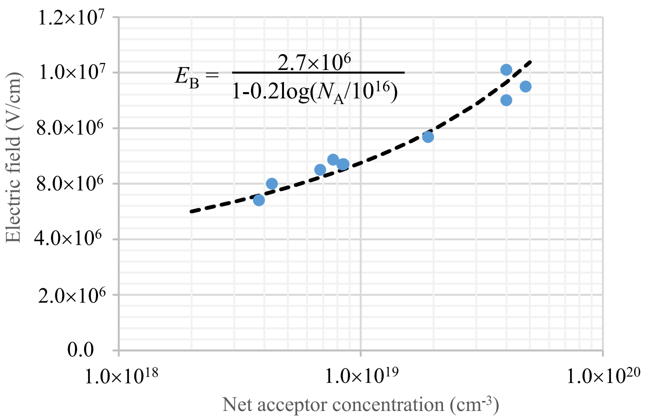

Fig. 7. (Color online) Dependence of breakdown field of the p^+-NiO/n^+-Ga_2O_3 diode on N_A of NiO layer. The breakdown field might correspond to the E_C of NiO layers.

$$E_C = \frac{2.7 \times 10^6}{1 - 0.2 \log (N_A/10^{16})}. \qquad (2)$$

The authors expressed the N_A dependence of E_C with an equation similar to that of SiC.[19,28,29] The values of 2.7×10^6 and 0.2 were determined by fitting the experimental data. The equation allows a deeper understanding of E_C in the NiO layer. The NiO layers with a high N_A concentration result in a high E_C. When the N_A is higher than 2.1×10^{19} cm^{-3}, the E_C is higher than 8 MV cm^{-1}, which is comparable to that of Ga_2O_3 (epilayers).[2] If high-voltage p^+-NiO/n^--Ga_2O_3 heterojunction diodes are considered, V_B can be limited by the E_C of a Ga_2O_3 epilayer, not by that of a highly doped NiO layer. Thus, the p^+-NiO/n^--Ga_2O_3 heterojunction devices can make full use of the potentials of Ga_2O_3. NiO is, therefore, a promising material to realize high-performance p-n heterojunction devices with Ga_2O_3.

As mentioned above, high-voltage (>1 kV) NiO/Ga_2O_3 diodes were reported by various groups[13–18] in the past. For example, a high V_B of 1860 V was reported.[13] The N_A of NiO used for the diode was 5.1×10^{17} cm^{-3}. According to the literature, the electric field around the p-n junction was calculated to be 3.5 MV cm^{-1} when V_B was applied. The reported E_B was comparable to the E_C of NiO calculated from Eq. (2) (4.1 MV cm^{-1}) for a N_A of 5.1×10^{17} cm^{-3}. In this case, the V_B of the heterojunction diode might be limited by NiO since the E_C of NiO was smaller than that of Ga_2O_3 due to lower N_A than 2.1×10^{19} cm^{-3}.

The E_B of the other high-voltage NiO/Ga_2O_3 heterojunction p-n diodes[14–18] is also discussed. The high E_B of 6.2–6.5 MV cm^{-1}[18] was reported for the heterojunction diodes using NiO layers with a "doping concentration" of 1×10^{18} cm^{-3}, which was obtained by Hall effect measurements. Unfortunately, the N_A of the NiO layers has not been clarified in the literature. However, the N_A of the NiO layer should be higher than the hole concentration. In the literature, the dopant for NiO was not clarified. If V_{Ni}, which has a large ionization energy of 0.39 eV,[21] was assumed to be utilized as an acceptor, N_A of the NiO layer may be four orders of magnitude higher than the doping concentration. This is because the ionization rate of V_{Ni} is lower than 0.1% due to the large ionization energy at the doping range at RT. Thus, the NiO/Ga_2O_3 heterojunction diodes in the literature may show a high breakdown field and may result in high V_B.

Next, we discuss the E_C of NiO in comparison with that of SiC. The E_C of NiO with a N_A of 1×10^{18} cm^{-3} is estimated to be 4.5 MV cm^{-1} from Eq. (2), while that of SiC is approximately 5 MV cm^{-1}.[19,28,29] The E_C tends to depend on the band gap.[2] Although the band gap of NiO (3.4–3.7 eV) is reported to be slightly higher than that of 4H-SiC (3.3 eV), the E_C of NiO was smaller than that of 4H-SiC. We anticipate the defects at the p-n junction (NiO/Ga_2O_3 interface defects) and/or in the NiO layers affect the E_C. The interface defects may generate electron-hole pairs under reverse bias conditions, which contribute to avalanche breakdown. Furthermore, carrier behavior such as impact ionization coefficient, mobility, and so on should be clarified for a better understanding of E_C of NiO. Although a single crystal was formed near the NiO/Ga_2O_3 interface as shown in Fig. 2, NiO layers also contain poly crystals near the interface (not shown), which can also reduce the E_C. The E_C can be improved by employing a high-quality NiO layer by exploring other methods such as the sol-gel method[30] or sputtering at a higher temperature.

4. Conclusions

In summary, the critical field, E_C, of NiO was investigated by using p^+-NiO/n^+-Ga_2O_3 heterojunction diodes. The N_A of NiO layers was controlled in the range from 1.0×10^{18} cm^{-3} to 4.8×10^{19} cm^{-3} by changing the Li concentration of NiO sputtering targets. The E_C of NiO, which was estimated by device simulation using N_A and V_B obtained from C–V and reverse I–V characteristics, depended on the N_A and ranged from 5.4 to 10.1 MV cm^{-1}. High E_C of NiO could be realized for highly doped NiO. The NiO can be one of the promising p-type oxides to realize high-power p-n heterojunction devices with Ga_2O_3.

Acknowledgments

The authors thank Dr. Y. Nagasato and Dr. T. Koyama at MIRISE Technologies Corporation and Dr. D. Banerjee at Toyota Motor North America, Inc. for helpful discussions.

1) H. H. Tippins, Phys. Rev. **140**, A316 (1965).
2) M. Higashiwaki, K. Sasaki, A. Kuramata, T. Masui, and S. Yamakoshi, Appl. Phys. Lett. **100**, 013504 (2012).
3) A. Kuramata, K. Koshi, S. Watanabe, Y. Yamaoka, T. Masui, and S. Yamakoshi, Jpn. J. Appl. Phys. **55**, 1202A2 (2016).
4) S. J. Pearton, J. Yang, P. H. Cary IV, F. Ren, J. Kim, M. J. Tadjer, and M. A. Mastro, Appl. Phys. Rev. **5**, 011301 (2018).
5) S. J. Pearton, F. Ren, M. Tadjer, and J. Kim, J. Appl. Phys. **124**, 220901 (2018).
6) N. Suzuki, S. Ohira, M. Tanaka, T. Sugawara, K. Nakajima, and T. Shishido, Physical Status Solidi (C) **4**, 2310 (2007).
7) M. Baldini, M. Albrecht, A. Fiedler, K. Irmscher, R. Schewski, and G. Wagner, ECS J. Solid State Sci. Technol. **6**, Q3040 (2017).
8) A. Kyrtsos, M. Matsubara, and E. Bellotti, Appl. Phys. Lett. **112**, 032108 (2018).
9) J. B. Varley, A. Janotti, C. Franchini, and C. G. Van de Walle, Phys. Rev. B **95**, 075208 (2017).
10) T. Gake, Y. Kumagai, and F. Oba, Phys. Rev. Mater. **3**, 044603 (2019).
11) F. P. Koffyberg and F. A. Benko, J. Electrochem. Soc. **128**, 2476 (1981).

12) Y. Kokubun, S. Kubo, and S. Nakagomi, Appl. Phys. Express **9**, 091101 (2016).
13) H. H. Gong, X. H. Chen, Y. Xu, F. –F. Ren, S. L. Gu, and J. D. Ye, Appl. Phys. Lett. **117**, 022104 (2020).
14) W. Hao, Q. He, K. Zhou, G. Xu, W. Xiong, X. Zhou, G. Jian, C. Chen, X. Zhao, and S. Long, Appl. Phys. Lett. **118**, 043501 (2021).
15) H. H. Gong et al., Appl. Phys. Lett. **118**, 212102 (2021).
16) Y. Wang et al., IEEE Trans. Power Electron. **37**, 4 (2022).
17) F. Zhou et al., IEEE Trans. Power Electron. **37**, 1223 (2022).
18) J. Zhang et al., Nature Commun. **13**, 3900 (2022).
19) T. Kimoto, Jpn. J. Appl. Phys. **54**, 040103 (2015).
20) W.-L. Jang, Y.-M. Lu, W.-S. Hwang, and W.-C. Chen, J. Eur. Ceram. Soc. **30**, 503 (2010).
21) K. O. Egbo, C. E. Ekuma, C. P. Liu, and K. M. Yu, Phys. Rev. Mater. **4**, 104603 (2020).
22) M. Passlack, N. E. J. Hunt, E. F. Schubert, G. J. Zydzik, M. Hong, J. P. Mannaerts, R. L. Opila, and R. J. Fischer, Appl. Phys. Lett. **64**, 2715 (1994).
23) K. V. Rao and A. Smakula, J. Appl. Phys. **36**, 2031 (1965).
24) F. Vera, R. Schrebler, R. Schrebler, E. Muñoz, C. Suarez, P. Cury, H. Gómez, R. Córdova, R. E. Marotti, and E. A. Dalchiele, Thin Solid Films **490**, 182 (2005).
25) Y. M. Lu, W. S. Hwang, and J. S. Yang, Surf. Coat. Technol. **155**, 231 (2002).
26) D. Kawade, S. F. Chichibu, and M. Sugiyama, J. Appl. Phys. **116**, 163108 (2014).
27) M. Mohamed, K. Irmscher, C. Janowitz, Z. Galazka, and R. Fornari, Appl. Phys. Lett. **101**, 132106 (2012).
28) A. O. Konstantinov, Q. Wahab, N. Nordell, and U. Lindefelt, Appl. Phys. Lett. **71**, 90 (1997).
29) H. Niwa, J. Suda, and T. Kimoto, IEEE Trans. Electron Devices **62**, 3326 (2015).
30) S. Nakagomi, T. Yasuda, and Y. Kokubun, Phys. Status Solidi B **257**, 1900669 (2020).

